# Synthesis, structure, and magnetic properties of a family of copper(II) complexes and salts of isoquinoline: $(isoquinoline)_nCu(X)_2$ [X=Cl, Br] and $(isoquinolinium)_2CuX_4(H_2O)_n$ [X= Cl, Br; n= 0,1]

Alistair D. Richardson,[a] Tyler J. Zirkman,[a] Michael T. Kebede,[a] Christopher P. Landee,[b] Melanie Rademeyer[c] and Mark M. Turnbull[a*]

[a] Carlson School of Chemistry and Biochemistry and [b]Department of Physics, Clark University, Worcester, MA 01610 USA. [c] Department of Chemistry, University of Pretoria, Pretoria, South Africa.

**Abstract**: The compounds $(iQuin)_2CuX_2$ (X = Br (**1**), Cl (**2**)), $(iQuinH)_2CuBr_4 \cdot H_2O$ (**3**) and two polymorphs of $(iQuinH)_2CuCl_4$ (**4**, **5**) (iQuin = isoquinoline) have been prepared and studied via X-ray crystallography and variable temperature magnetic susceptibility measurements. Compound **1** crystallizes in the monoclinic space group $P2_1/n$ while **3**, **4** and **5** all crystallize in the triclinic space group P-1. Magnetic susceptibility measurements for **1** are best fit by an antiferromagnetic alternating chain model (J = -56.6(2) K, J' = 5.1(8) K) although the crystal structure suggests a uniform chain. Compound **2** is well described as an isolated uniform antiferromagnetic chain (J = -25.6(1) K), while **3** agrees well with the antiferromagnetic rectangular model (J = -5. 03(2) K, J' = -1.0(1) K). The two polymorphs, **4** and **5**, exhibit distinctly different behavior as **4** is well described by the 2D-square antiferromagnetic layer model (J = -4.24(2) K), but **5** crystallizes as well isolated magnetic dimers (J = -15.8(1) K). Magnetic superexchange is proposed to occur via either the bihalide or two-halide pathways. Finally, compound **6**, isoquinolinium tribromide) was isolated as a biproduct of the synthesis of **3** and was characterized via X-ray diffraction. The formation of the tribromide ion in situ provides support for the mechanism of electrophilic aromatic bromination reactions which have been previously observed in syntheses similar to that of **3**.

## Introduction

The field of molecular magnetism has erupted since the discovery of two-dimensional high-temperature, superconducting copper-oxide compounds.[1] Since then, the coordination chemistry and magnetism communities have been developing metal coordination compounds to better understand these superconducting systems.[2,3] In particular, several compounds of the general formula $L_nMX_n$ and $(LH)_n[MX]_n$ have been of interest as they may provide the same lattice type as is observed in the high $T_c$ superconductors, but with weaker magnetic exchange which allows for detailed study at accessible temperatures and magnetic fields .[4,5,6,7] These systems are particularly important for understanding magnetostructural correlations. Copper(II) is an attractive metal for study because of its $d^9$ electron configuration and spin of ½, making it a quantum system. With typical g-values near 2.1, copper's magnetic properties can frequently be treated as Heisenberg-like.[8] While the halide ions are typically responsible for the magnetic exchange observed between copper ions in these systems,[9] the ancillary species affect how the complexes pack into a three-dimensional lattice and they influence the geometry of the copper coordination sphere through their packing. Both of these factors impact the potential magnetic superexchange pathways and the resulting sign and strength of the magnetic exchange. The geometry of a four coordinate Cu(II) species ranges from tetrahedral[10] to square planar,[11] with a distorted tetrahedral geometry being the most common. The ancillary ligands may also isolate the copper(II) ion-containing species creating low-dimensional magnetic lattices.[12] The synthesis

and analysis of families of such complexes have become important to provide a better understanding of how different compositions and structures may control magnetic behavior.[13,14]

There has been extensive research into metal halide complexes and salts with quinoline (Quin) and substituted quinoline molecules as ligands or cations (in their protonated form, QuinH), of the general form $(Quin)_2MX_2$ and $(QuinH)_2[MX_4]$, and into the relationship between the structures of those compounds and their magnetic behavior.[15,16,17,18,19,20,21,22] Quinoline is a useful ligand due to its size, which can effectively separate the magnetic species into a variety of lattice types. Ideally, this keeps the magnetic exchange in one or two dimensions, leading to changes in the nature of the magnetic interactions. Two quinolinium tetrabromocuprate salts, $(QuinH)_2CuBr_4 \cdot (H_2O)_n$ (n=0,2), have been reported.[15] In addition, several quinolinium tetrachlorometalates of the form $(QuinH)_2MCl_4 \cdot (H_2O)_n$ (n=0,2), have been produced with copper,[16] zinc,[17] and iron. [21] A range of substituted quinoline metal complexes has also been reported. For example, 4- and 6-methylquinolinium chlorochromates,[22] as well as 2-[19] and 8-[20] methylquinolinium iron halide salts are known as is an iron(III) chloride salt of 4-amino-2-methylquinolinium.[18]

Isoquinoline (iQuin), however, has received limited attention. There has been some research into the magnetostructural correlations of isoquinoline, and other *N*-heterocyclic ligands, in nickel (II) complexes.[23,24] The magnetic properties of copper(II) imide complexes with isoquinoline as a ligand have also been studied.[25] We were interested in examining how the change in position of the nitrogen atom in isoquinoline would affect the structure and magnetic exchange properties of copper(II) halide complexes and salts relative to what is observed in the quinoline analogs and thus have begun a study of these materials. Herein, we report the synthesis, structure and temperature dependent magnetic properties of $CuX_2(iQuin)_2$ [X= Br (**1**), Cl (**2**)], and $(iQuinH)_2CuX_4 \cdot (H_2O)_n$ (X= Br, n = 1 (**3**); X = Cl, n = 0, (**4** and **5**)]. Further, we report the serendipitous synthesis and crystal structure of isoquinolinium tribromide (iQuinH $Br_3$) (**6**).

## Experimental

### Materials

Copper(II) chloride dihydrate was purchased from Allied Chemical Corporation. Copper(II) bromide, hydrobromic acid, and dimethyl sulfoxide (DMSO) were purchased from Aldrich Chemical Company. Isoquinoline was purchased from Acros Chemical Company. Hydrochloric acid was purchased from Fisher Scientific. All chemicals were used as received. Distilled water was used in all syntheses. IR spectra were recorded via ATR on a Perkin-Elmer Spectrum 100. X-Ray powder diffraction experiments were carried out on a Bruker AXS-D8 Focus X-ray Powder Diffractometer. Elemental analyses were carried out by Marine Science Institute, University of California, Santa Barbara CA 93106.

### Synthesis

Bis(isoquinoline)dibromocopper(II) (**1**)

Isoquinoline (0.1303 g, 1.01 mmol) was dissolved in ca. 3 ml of dimethyl sulfoxide (DMSO), yielding a pale yellow solution. $CuBr_2$ (0.1117 g, 0.499 mmol) was dissolved in ca. 3 ml of

DMSO with warming, yielding a dark-brown, nearly black solution. Addition of the isoquinoline solution to the $CuBr_2$ solution produced a bright green solution which was left at room temperature. After a few hours, the solution turned from bright green to a darker green. After nearly a week, clusters of forest-green acicular crystals formed. The crystals were isolated via vacuum filtration and allowed to air-dry to give 0.0541 g (22.5%). IR (ν in $cm^{-1}$): 3052 (w), 1634 (s), 1597 (w), 1500 (m), 1389 (s), 1280 (s), 1260 (w), 1241 (w), 1214( m), 1179 (w), 1149 (w), 1043 (s), 1017 (m), 970 (w), 960 (s), 932 (s), 865 (m), 838 (s), 825 (s), 772 (m), 745 (s), 738 (s), 636 (s), 585 (w). CHN found (calculated): C: 44.9 (44.9) H: 2.88 (2.93) N: 5.56 (5.82)

Bis(isoquinoline)dichlorocopper(II) (**2**)
Isoquinoline (0.128 g, 0.99 mmol) was dissolved in 5 mL of 50:50 methanol:water yielding a pale yellow solution. $CuCl_2 \cdot 2H_2O$ (0.087 g, 0.51 mmol) was dissolved in 5 mL of 50:50 methanol:water yielding a light-blue solution. Addition of the isoquinoline solution to the $CuCl_2 \cdot 2H_2O$ solution produced an immediate light-blue precipitate. After all the isoquinoline was added, the mixture was stirred until uniform and the precipitate was isolated through vacuum filtration, washed with additional 50:50 methanol:water and allowed to air dry to give 0.160 g (81.9%). IR (ν in $cm^{-1}$): 3062 (w), 1635 (m), 1604 (w), 1502 (m), 1389 (m), 1276 (m), 1215 (w), 1181 (w), 1143 (w), 1049 (m), 1014 (w), 962 (w), 928 (w), 860 (m), 825 (s), 815 (s), 772 (w), 750 (w), 738 (s), 636 (s). CHN found (calculated): C: 54.9 (55.1), H: 3.52 (3.57) N: 7.18 (7.13).
A similar synthesis was performed in dimethyl sulfoxide (DMSO) to produce the same compound. Isoquinoline (0.130 g, 1.01 mmol) was dissolved in 5 mL of dimethyl sulfoxide (DMSO), yielding a pale-yellow solution. $CuCl_2 \cdot 2H_2O$ (0.087 g, 0.51 mmol) was dissolved in 6.5 mL of DMSO with warming, yielding a light-green solution. Addition of the isoquinoline solution to the $CuCl_2 \cdot 2H_2O$ solution produced a darker-green solution, which was left at room temperature. After a few hours, very thin, small, light-blue crystals formed on the surface of the solution. The following day, large clumps of acicular crystals had formed. These pale blue crystals were isolated using vacuum filtration, washed with methanol, and allowed to air dry to give 0.093 g (47.0%). Powder X-ray diffraction showed the crystals to be the same as the powder above, but we were unsuccessful at obtaining single crystal diffraction data after repeated attempts.

Bis(isoquinolinium) tetrabromocuprate(II) monohydrate (**3**)
Isoquinoline (0.2487g, 1.92 mmol) was dissolved in 3 ml of $H_2O$ and 2.2 ml of HBr (8.9 M), which yielded a golden-brown solution. $CuBr_2$ (0.2244 g, 1.00 mmol) was dissolved in 12 ml of $H_2O$ yielding a dark brown, nearly black, solution. Addition of the isoquinoline solution to the $CuBr_2$ solution produced a sky-blue solution, which was left to evaporate at room temperature. After a week, large square purple crystals were isolated from the resulting purple reaction mixture through vacuum filtration and allowed to air dry to give 0.496 g (80%). IR (ν in $cm^{-1}$): 3249 (w), 3048 (m), 1646 (s), 1609 (s), 1586 (w), 1539 (m), 1493 (w), 1406 (w), 1392 (s), 1282 (m), 1272 (m), 1269 (m), 1256 (m), 1205 (w), 1155 (s), 1032 (w), 918 (m), 878 (m), 828 (s), 808 (s), 771 (w), 768 (m), 748 (s), 625 (w), 621 (w). CHN found (calculated) for $C_{18}H_{18}N_2OCuBr_4$: C: 32.6 (32.7),H: 2.47 (2.72), N: 4.27 (4.24).

The filtrate from this reaction was left partially covered to continue to evaporate at room temperature. After ten months, small orange crystals appeared, along with small traces of purple crystals of **3**. The orange crystals were physically separated from the purple crystals under a microscope (0.003 g) and proved to be isoquinolinium tribromide (**6**) by single crystal X-ray analysis. IR (ν in $cm^{-1}$): 3133 (w), 3046 (m), 1639 (s), 1607 (s), 1580 (m), 1537 (s), 1486 (m), 1404 (m), 1392 (s), 1371 (m), 1278 (m), 1253 (s), 1196 (w), 1159 (s), 1138 (w), 1030 (m), 1015 (m), 998 (w), 985 (w), 973 (w), 949 (w), 897 (w), 856 (m), 817 (s), 805 (s), 766 (s), 750 (s), 629 (w), 617 (w).

Bis(isoquinolinium) tetrachlorocuprate(II) (**4**) and (**5**)
Isoquinoline (0.2505 g, 1.94 mmol) was dissolved in 3.4 ml of $H_2O$ and 2 mL of HCl (conc.) yielding a pale-yellow solution. $CuCl_2 \cdot 2H_2O$ (0.1733 g, 1.01 mmol) was dissolved in 10 mL of $H_2O$ yielding a light-blue solution. Addition of the isoquinoline solution to the $CuCl_2(H_2O)_2$ solution produced a turquoise solution, which was left to evaporate at room temperature. After two weeks large square orange crystals (**4**), as well as small square yellow crystals (**5**), formed. If left in the mother liquor, the orange crystals slowly dissolve, giving way to more yellow crystals. All crystals were isolated using vacuum filtration, and the two polymorphs were manually separated under a microscope. Total yield 0.165 g (36.5%); 0.068 g (15.0%) orange, 0.097 g (21.5%) yellow. IR (ν in $cm^{-1}$): (yellow, **5**): 3046 (m), 2916 (w), 1642 (m), 1609 (m), 1582 (w), 1536 (w), 1488 (m), 1395 (m), 1372 (m), 1279 (w), 1258 (w), 1199 (w), 1166 (w), 1033 (w), 1017 (w), 975 (w), 860 (m), 817 (s), 769 (m), 751 (m), 620 (w). (orange, **4**): 3021 (m), 2871 (m), 1645 (m), 1611 (m), 1586 (w), 1552 (w), 1490 (w), 1411 (w), 1394 (m), 1374 (m), 1290 (w), 1275 (w), 1258 (w), 1201 (w), 1158 (w), 1017 (w), 979 (w), 912 (w), 861 (m), 823, 802 (m), 769 (m), 757 (s), 631 (w), 620 (w). CHN found(calculated): (yellow, **5**) C: 46.6 (46.4), H: 3.48 (3.46), N: 6.05 (6.01). CHN found (calculated): (orange, **4**) C: 46.3(46.4), H: 3.34 (3.46), N: 5.96 (6.01)

**Single crystal X-ray diffraction**
The X-ray diffraction data for all compounds were collected using a Bruker D8 Venture diffractometer, with a Photon 100 CMOS detector, at 150(2) K, employing a combination of ϕ and ω scans. Monochromatic MoKα radiation with a wavelength λ of 0.71073 Å, from an IμS source, was used as the irradiation source. Data reduction and absorption corrections were performed using SAINT+[26] and SADABS[27]. The structures were solved by direct methods and refined using SHELX97[28].

All non-hydrogen atoms were refined anisotropically. Hydrogen atoms bonded to carbon atoms were added in calculated positions and refined using a riding model with fixed isotropic thermal parameters. Hydrogen atoms bonded to nitrogen and oxygen atoms were located in the difference map and their positions were refined with fixed isotropic thermal parameters. Crystallographic information and details of the data collection can be found in Table 1. CIF files have been deposited with the CCDC as #1588031-1588035.

**Magnetic Susceptibility**

Magnetic data were collected using a Quantum Design MPMS-XL SQUID magnetometer. Crystals were finely ground and packed into gelatin capsules which were then mounted into straws. The moment was measured using magnetic fields from 0 to 50 kOe at 1.8 K. Several data points were collected as the field returned to 0 kOe in order to check for hysteresis effects; none were observed. Magnetization was measured from 1.8 to 310 K in a 1 kOe field. The magnetization of the gelatin capsule and sample holder were measured independently and used as the background signal. The data was also corrected for the temperature independent paramagnetism of the Cu(II) ions ($60 \times 10^{-6}$ emu $mol^{-1}$ $Oe^{-1}$) and for the diamagnetism of the constituent atoms estimated from Pascal's constants.[8] All data were fit using the Hamiltonian $\hat{H} = -\Sigma_{A,B} J_{AB} \hat{S}_A \cdot \hat{S}_B$ and equations taken from Ref. 26.[26]

**Results**

**Synthesis**

The reaction of $CuBr_2$ with isoquinoline in DMSO yielded $CuBr_2(iQuin)_2$ (**1**). Similarly, the reaction of $CuCl_2 \cdot 2H_2O$ with isoquinoline in DMSO yielded $CuCl_2(iQuin)_2$ (**2**). Bulk synthesis of both materials can be done in 50:50 methanol:water generating an immediate precipitate, in high yield, which was identical to the crystalline material according to IR and powder X-ray diffraction. Reaction at room temperature in DMSO for **1** gave crystals suitable for single crystal X-ray diffraction. Although crystals of **2** could also be grown from DMSO, they were not suitable for single-crystal analysis. Multiple attempts to grow X-ray quality crystals of **2** from a variety of solvents were unsuccessful. Yields ranged from 22-82%.

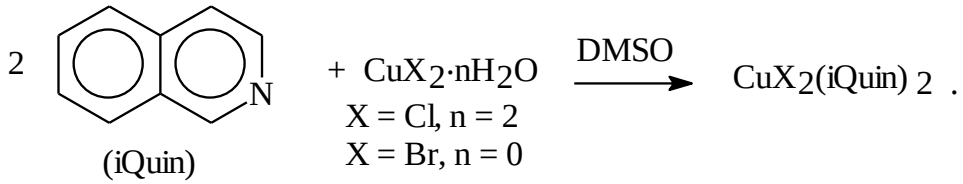


Figure 1. Preparation of **1** (X = Br) and **2** (X = Cl).

The reaction of $CuX_2 \cdot nH_2O$ with isoquinoline in acidic aqueous solution yielded three different copper-containing products: $(iQuinH)_2CuBr_4 \cdot H_2O$ (**3**), $(iQuinH)_2CuCl_4$ (**4**) and its polymorph $(iQuinH)_2CuCl_4$ (**5**). Through slow evaporation at room temperature, crystals suitable for single crystal X-ray diffraction were obtained for all three. Yields ranged from 36-80%. A few crystals of isoquinolinium tribromide (iQuinH $Br_3$, **6**) were isolated as a by-product of the synthesis of **3** (*vide supra*).

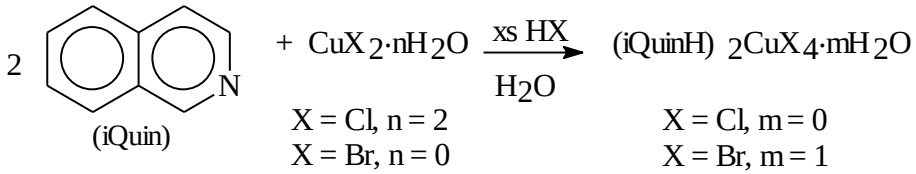


Figure 2. Preparation of **3** (X = Br), **4** and **5** (X = Cl).

Table 1 – Cell constants and X-ray data collection parameters for **1**, **3**, **4**, **5** and **6**.

| Compound | **(1)** | **(3)** | **(4)** | **(5)** | **(6)** |
|---|---|---|---|---|---|
| Formula | $C_{18}H_{14}$ $Br_2CuN_2$ | $C_{18}H_{18}Br_4CuNO$ | $C_9H_8$ $Cl_2$ $Cu_{0.5}N$ | $C_{18}H_{16}Cl_4CuN_2$ | $C_{18}H_{16}$ $Br_6N_2$ |
| Mol. Wt. | 481.67 | 661.49 | 232.83 | 465.67 | 739.79 |
| Temp (K) | 150(2) | 150(2) | 150(2) | 150(2) | 150(2) |
| Crystal System | Monoclinic | Triclinic | Triclinic | Triclinic | Triclinic |
| Space Group | P2(1)/n | P-1 | P-1 | P-1 | P-1 |
| Unit cell: a(Å)<br>b(Å)<br>c(Å)<br>α(°)<br>β(°)<br>γ(°) | 12.5169(5)<br>4.04230(10)<br>16.7677(6)<br>90.00<br>100.409(2)<br>90.00 | 7.3862(7)<br>7.8693(8)<br>18.2890(18)<br>86.868(2)<br>89.476(3)<br>89.772(18) | 7.6828(2)<br>7.7078 (2)<br>16.3180(5)<br>101.5850(10)<br>96.2120(10)<br>91.4290(10) | 7.257(10)<br>8.004(10)<br>17.06(2)<br>81.97(5)<br>84.70(6)<br>83.20(6) | 7.5632(4)<br>10.3876(5)<br>14.5173(7)<br>96.604(2)<br>92.206(2)<br>108.636(2) |
| Volume ($Å^3$) | 834.43(5) | 1061.49(18) | 939.99(4) | 971(2) | 1070.12(9) |
| Z | 2 | 2 | 2 | 2 | 2 |
| Density ($Mg/m^3$) | 1.917 | 2.070 | 1.645 | 1.592 | 2.296 |
| Abs. Coeff ($mm^{-1}$) | 6.096 | 8.567 | 1.734 | 1.677 | 8.492 |
| Cryst. Dim. ($mm^3$) | 0.14 x 0.05 x 0.03 | 0.26 x 0.24 x 0.22 | 0.26 x 0.25 x 0.22 | 0.23 x 0.23 x 0.21 | 0.32x 0.29 x 0.28 |
| θ range (°) | 2.24 to 26.61 | 2.59 to 32.69 | 2.70 to 45.31 | 2.42 to 22.62 | 2.36 to 29.71 |
| Index ranges | $-15 \le h \le 15$<br>$-5 \le k \le 5$<br>$-21 \le l \le 21$ | $-11 \le h \le 11$<br>$-11 \le k \le 11$<br>$-27 \le l \le 27$ | $-11 \le h \le 14$<br>$-15 \le k \le 15$<br>$-16 \le l \le 32$ | $-7 \le h \le 7$<br>$-8 \le k \le 8$<br>$-18 \le l \le 18$ | $-10 \le h \le 10$<br>$-14 \le k \le 14$<br>$-20 \le l \le 20$ |
| Total Rlfn | 29113 | 33363 | 11677 | 4297 | 51589 |
| Ind. Rlfn ($R_{int}$) | 1736(0.0572) | 7782 (0.0620) | 9288 (0.0163) | 2344 (0.0339) | 6076(0.1249) |
| Max(min) trans. | 0.8430(0.4824) | | | 0.7185(0.6979) | 0.1471(0.1241) |
| Data/restr./param. | 1736 / 0 / 106 | 7782 / 0 / 247 | 9288 / 1 / 232 | 2344 / 0 / 232 | 6076 / 0 / 241 |
| GooF | 1.121 | 1.146 | 1.061 | 1.065 | 1.022 |
| Fin. $R_1(wR_2)I>2\sigma$ | 0.0234(0.0459) | 0.0520(0.1146) | 0.0460(0.0982) | 0.0406(0.1025) | 0.0488(0.1019) |
| Fin. $R_1(wR_2)$all | 0.0342(0.0.492) | 0.0745(0.1244) | 0.0721(0.1094) | 0.0600(0.1113) | 0.0861(0.1163) |
| Peak(hole) ($e/Å^3$) | 0.376(-0.842) | 1.910(-1.115) | 1.169 (-0.520) | 0.409(-0.317) | 0.887(-1.595) |

Table 2 - Bond lengths (Å) and angles (°) for **1**, **3**, **4**, and **5**.

| Compound | (**1**) | (**3**) | (**4**) | (**5**) |
|---|---|---|---|---|
| Cu1-X1 | 2.4311(3) | 2.3863(7) | 2.2314(5) | 2.232(3) |
| Cu1-X2 | | 2.3755(7) | 2.2305(4) | 2.231(3) |
| Cu1-X3 | | 2.3640(7) | 2.2561(4) | 2.242(3) |
| Cu1-X4 | | 2.3795(7) | 2.2554(4) | 2.225(3) |
| Cu1-N1 | 2.000(2) | | | |
| N12-C11 | 1.309(3) | 1.310(7) | 1.323(3) | 1.298(7) |
| N12-C13 | 1.371(3) | 1.373(8) | 1.366(2) | 1.331(7) |
| N22-C21 | | 1.322(6) | 1.323(3) | 1.315(7) |
| N22-C23 | | 1.362(7) | 1.360(3) | 1.342(8) |
| | | | | |
| X1-Cu1-X2 | | 125.62(3) | 96.04(2) | 98.51(90) |
| X1-Cu1-X3 | | 99.99(3) | 144.234(19) | 98.12(9) |
| X1-Cu1-X4 | | 99.31(3) | 93.804(19) | 132.17(9) |
| X2-Cu1-X3 | | 99.53(3) | 96.595(17) | 136.81(8) |
| X2-Cu1-X4 | | 101.63(3) | 144.874(17) | 97.59(9) |
| X3-Cu1-X4 | | 134.71(3) | 94.790(16) | 100.09(11) |
| Br1*-Cu1-Br1 | 180 | | | |

| | | | | |
|---|---|---|---|---|
| N12*-Cu1-Br1 | 90.82(6) | | | |
| N12-Cu1-Br1 | 89.18(6) | | | |
| N12-Cu1-N12* | 180 | | | |
| C11-N12-C13 | 118.3(2) | 123.6(4) | 123.14(16) | 123.0(5) |
| N12-C11-C20 | 123.7(2) | 120.3(5) | 120.16(14) | 121.4(5) |
| C14-C13-N12 | 122.6(2) | 118.5(5) | 119.65(17) | 119.9(6) |
| N22-C21-C30 | | 120.0(4) | 119.94(17) | 119.5(5) |
| C21-N22-C23 | | 123.4(4) | 123.10(16) | 122.0(5) |
| C24-C23-N22 | | 119.6 (4) | 120.18(18) | 121.2(6) |

* = -x+2, -y+1, -z+1

Table 3 – Hydrogen bond parameters for **3**, **4**, **5** and **6** (Å, °)

| Compound | D-H...A | d(D-H) | d(H...A) | d(D...A) | <(DHA) |
|---|---|---|---|---|---|
| **3** | N(12)-H(12)…Br(3)#1 | 0.76(3) | 2.29(3) | 2.710(2) | 115(2) |
| | N(22)-H(22)…O(1)#2 | 0.76(3) | 2.43(3) | 3.005(2) | 133(2) |
| | O(1)-H(1A)...Br(2)#3 | 0.85(2) | 2.05(2) | 2.795(2) | 146(2) |
| | O(10-H(1B)…Br(1) | 0.83(8) | 2.60(8) | 3.328(4) | 147(6) |
| **4** | N(12)-H(12)…Cl(3)#4 | 0.834(16) | 2.347(17) | 3.1594(16) | 165(2) |
| | N(22)-H(22)…Cl(4)#5 | 0.84(3) | 2.55(3) | 3.2695(17) | 146 (3) |
| | N(22)-H(22)…Cl(4)#5 | 0.84(3) | 2.73(3) | 3.3730(18) | 135(3) |
| **5** | N(12)-H(12)…Cl(2)#6 | 0.90(5) | 2.44(6) | 3.152(6) | 136(5) |
| | N(12)-H(12)…Cl(2)#6 | 0.90(5) | 2.59(6) | 3.324(7) | 140(5) |
| | N(22)-H(22)…Cl(1)#7 | 0.93(6) | 2.25(6) | 3.102(2) | 152(5) |
| | N(22)-H(22)…Cl(3)#7 | 0.93(6) | 2.87(6) | 3.504(7) | 126(4) |
| **6** | N(12)-H(12)…Br(6)#8 | 0.86(4) | 2.65(4) | 3.330(4) | 137(4) |
| | N(12)-H(12)…Br(3)#9 | 0.86(4) | 2.96(4) | 3.587(4) | 132(4) |
| | N(22)-H(22)…Br(3)#10 | 0.87(4) | 2.79(5) | 3.484(4) | 138(4) |
| | N(22)-H(22)…Br(6) | 0.87(4) | 2.82(4) | 3.433(4) | 129(2) |

Symmetry transformations used to generate equivalent atoms: #1 x-1,y-1,z #2 x,y-1,z #3 x+1,y,z #4 x-2,y,z-1 #5-x,-y+1,-z #6 -x,-y+2,-z #7 -x,-y+1,-z+1 #8 -x+2,-y+2,-z #9 -x+2,-y+1,-z+1 #10 x-1,y,z

**Crystal Structure analysis**

Compound **1** crystallized in the monoclinic space group $P2_1/n$ while compounds **3-6** crystallized in the triclinic space group *P*-1. Crystallographic data for all compounds are given in Table 1. Selected bond lengths and angles are given in Table 2. Hydrogen bonding parameters are given in Table 3.

X-ray structure of bis(isoquinoline)dibromocopper(II**) (1)**

The asymmetric unit contains a Cu(II) ion coordinated by one bromide ion and one isoquinoline molecule. Figure 3 shows the molecular unit. The copper ion sits on a crystallographic inversion center with the N12-Cu1-N12A and Br1-Cu1-Br1A bond angles equal to 180˚, as required by symmetry. The N12-Cu1-Br1 bond angle is 89.18(6)°; the geometry is only slightly distorted from square planar.

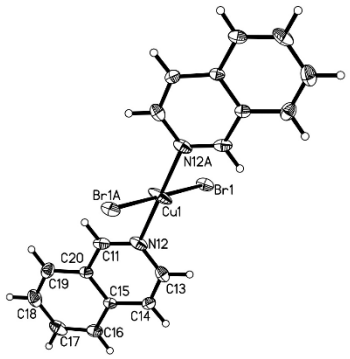


Figure 3 The thermal ellipsoid plot of **1** showing 50% probability ellipsoids. The asymmetric unit and the copper coordination sphere are labeled. Hydrogen atoms are not labeled for clarity.

The conformation of the isoquinoline rings is anti, also as required by symmetry. Further, each isoquinoline ring is canted 61.3° from the copper coordination plane. The bond angles and bond lengths of the isoquinoline ring are unremarkable in comparison to those in similar compounds such as chloro-isoquinoline-bis(triphenylphosphine)copper(I),[27] diaqua-bis(isoquinoline) copper(II) perchlorate[28] and trans-bis(aceto)diaqua-bis(isoquinoline)cobalt(II).[29] The isoquinoline ring is highly planar, with a mean deviation of its constituent atoms of 0.007 Å. The molecular units pack into bihalide bridged chains that run parallel to the *b*-axis (Fig 4). The copper-bromide bond is 2.431(3) Å while the long copper…bromide contact is 3.376(4) Å. The Cu1A-Br1C…Cu1 angle is 86.6(3)° while the Br1C…Cu1-Br1 angle is supplementary (93.4(3)°).

The bond angles and lengths of the bihalide bridged chain are comparable to those of *catena*-(bis($\mu_2$-bromo)-bis(3-pyridinol)copper(II))[30] and catena-(bis($\mu_2$-bromo)-3,5-dimethylpyridine-copper(II)).[31] The closest Br…Br interaction between chains is greater than 8 Å (Fig. 5), suggesting that the chains are extremely well isolated.

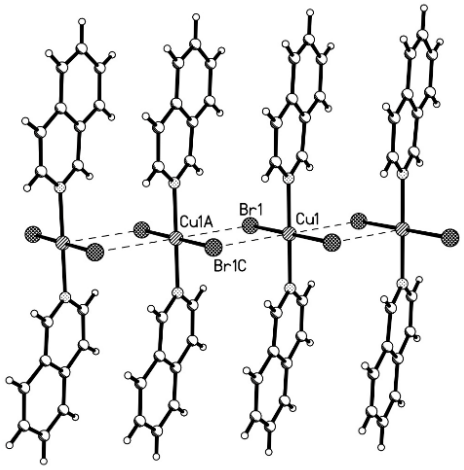


Figure 4 Bihalide bridged chain structure of **1.**

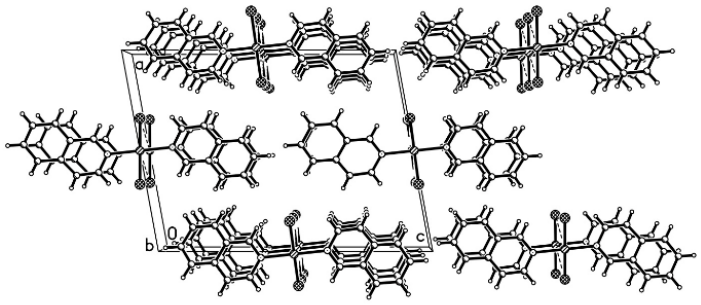


Figure 5 Packing diagram of **1**, viewed parallel to the *b*-axis, illustrating the isolation of the chains.

X-ray powder diffraction of bis(isoquinoline)dichlorocopper(II) (**2**)

Attempts to prepare crystals of **2** suitable for single-crystal study were unsuccessful and thus we compared the X-ray powder diffraction data of **2** to the cell parameters obtained from the structure of **1** since it was reasonable that the two compounds could be closely related. The presence of a few additional peaks at low angle suggested that the structure might be lower symmetry and the space group was lowered to P-1 from $P2_1/n$ and the *b*-axis length was doubled to correspond with the reduced symmetry. A satisfactory fit was obtained with cell parameters: a = 8.1729 Å, b = 12.7244 Å, c = 16.5049 Å. α = 88.651°, β = 96.641°, γ = 95.820°. The close correspondence between the cell parameters suggests that the compounds likely have similar structures, as expected, but different arrangements in the crystal lattice.

X-ray structure of bis(isoquinolinium)tetrabromocuprate(II) monohydrate (**3**)

The asymmetric unit of **3** contains two independent isoquinolinium ions, one tetrabromocuprate ion and a water molecule (Fig. 6). The mean trans angle (mta) at the Cu(II) ion is 130.12(3)° suggesting that the geometry of the $CuBr_4^{2-}$ anion is intermediate between tetrahedral and square planar as is common in tetrabromocuprate(II) compounds.[12] The four bromide ions are all independent (Table 1). Although the monohydrate complex with quinoline has not been reported, both bis(quinolinium) tetrabromocuprate(II) and bis(quinolinium) tetrabromcuprate(II) dihydrate are known.[15] The two isoquinolinium rings are hydrogen bonded, through the N-H hydrogen atom, to the $CuBr_4^{2-}$ ion (Table 3).

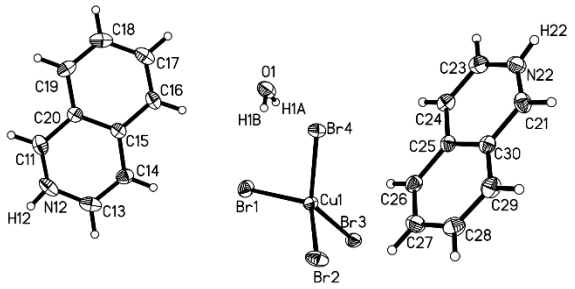


Figure 6 The thermal ellipsoid plot of **3** showing 50% probability ellipsoids. The asymmetric unit, the copper coordination sphere and hydrogen atoms in refined positions are labeled.

The water molecule also interacts with the $CuBr_4^{2-}$ ion through hydrogen bonds (Table 3). The bond angles and bond lengths of the isoquinolinium rings are unremarkable in comparison to those in similar compounds isoquinolinium tetrachloroironate(III)[32] and bis(isoquinolinium) tetrachlorozincate dihydrate.[32,33] The isoquinoline ring is again highly planar, with a mean deviation of its constituent atoms of 0.015 Å (N11 ring) and 0.022 Å (N22 ring). The planes of the isoquinoline rings are canted 61.9°, with respect to one another. The $CuBr_4^{2-}$ ions form a rectangular lattice through short bromide…bromide contacts which provide the magnetic superexchange pathway (Fig. 7). There are two unique halide-halide contacts, one at 3.880(1.2) Å (Br4…Br3D) and one at 4.151(1.5) Å (Br1…Br2A). Full details of the exchange pathways are given in Table 4. The packing diagram illustrates alternating layers of $CuBr_4^{2-}$ ions and isoquinolinium ions (Fig. 8).

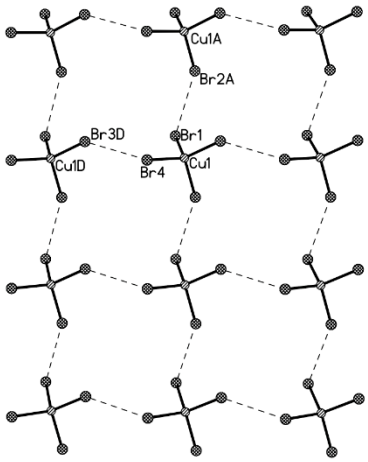


Figure 7 Rectangular lattice of $CuBr_4^{2-}$ ions, showing the proposed magnetic exchange pathway of **3** (viewed parallel to the *c*-axis).

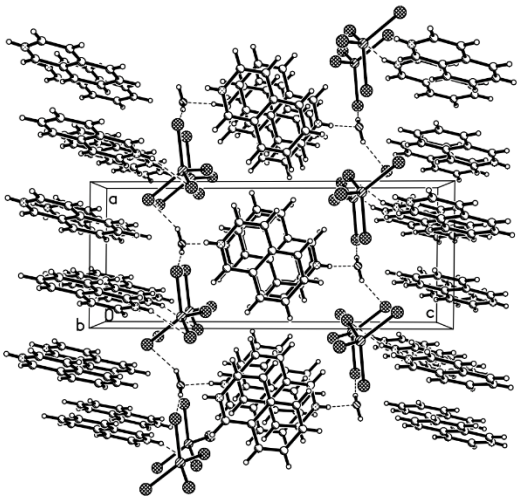


Figure 8 Packing diagram of **3** viewed along the *b*-axis**.**

Table 4 - Bi-halide (**1**) ($d_{X...Cu}$, $\theta_{Cu-X...Cu}$) and two-halide (**3**, **4**, **5**) ($d_{X...X}$, $\theta_{Cu-X...X}$, $\theta_{X...X-Cu}$, $\tau_{Cu-X...X-Cu}$) superexchange pathway parameters (Å, °). Compounds **3**-**5** each exhibit two different two-halide superexchange pathways which are listed separately.

| Compound | (**1**) | (**3**) | (**4**) | (**5**) |
|---|---|---|---|---|
| Cu1…Br1C | 3.376(0.4) | | | |
| Cu1-Br1…Cu1A | 86.6(3) | | | |
| | | | | |
| X…X | | 3.880(12) | 3.779(6) | 3.752(4) |
| Cu-X…X | | 137.9(3) | 139.2(2) | 175.0(1) |
| X…X-Cu | | 139.8(3) | 145.7(2) | 175.0(1) |
| Cu-X…X-Cu | | 108.5(7) | 121.5(2) | 180 |
| | | | | |
| X…X | | 4.151(1.5) | 3.852(7) | 4.709(7) |
| Cu-X…X | | 100.3(3) | 133.7(2) | 135.0(1) |
| X…X-Cu | | 143.4(3) | 144.1(2) | 87.3(1) |
| Cu-X…X-Cu | | 138.3(7) | 126.4(2) | 175.8(1) |

X-ray structure of bis(isoquinolinium)tetrachlorocuprate(II) (**4**)

The asymmetric unit of **4** contains two independent isoquinolinium ions and one tetrachlorocuprate ion (Fig. 9). The mta at the Cu(II) ion is 144.554(18)° showing that the geometry of the $CuCl_4^{2-}$ ion is intermediate between tetrahedral and square planar and further from tetrahedral than was observed in **3**. The four chloride ions are all independent (Table 2). Cu-Cl bond lengths of **4** are comparable to bis(8-methylquinolinium) tetrachlorocuprate(II),[20]

bis(2-methylquinolinium) tetrachlorocuprate(II),[34] and bis(quinolinium) tetrachlorocuprate(II) dihydrate.[16] Bond angles of **4**, with its highly distorted $CuCl_4^{2-}$ ion, do not compare to any of these structures. The two unique isoquinolinium rings hydrogen bond, through the N-H hydrogen, to the $CuCl_4^{2-}$ ion (Table 3). The bond angles and bond lengths of the isoquinolinium rings are unremarkable in comparison to those in (**3**). The isoquinoline rings are highly planar, with a mean deviation of constituent atoms of 0.003 Å (N12) and 0.006 Å (N22). The planes of isoquinoline rings are canted 89.7° with respect to one another. The $CuCl_4^{2-}$ ions form a rectangular lattice with short chloride…chloride contacts of 3.779(0.6) Å (Cl2G-Cl4A) and 3.852(0.7) Å (Cl1C-Cl3G) (Fig. 10). Full geometric parameters for the two-halide superexchange pathways are given in Table 4. The packing diagram illustrates alternating layers of $CuCl_4^{2-}$ ions and isoquinolinium ions (Fig. 11).

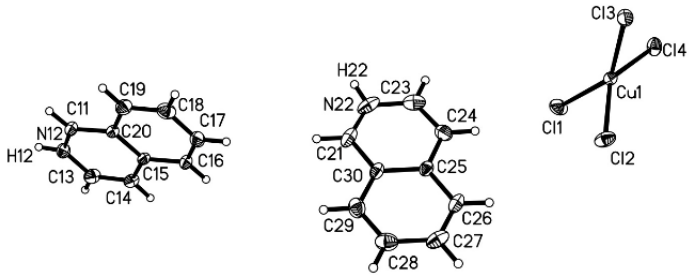


Figure 9 The thermal ellipsoid plot of **4** showing 50% probability ellipsoids. The asymmetric unit, the copper coordination sphere, and hydrogen atoms in refined positions are labeled.

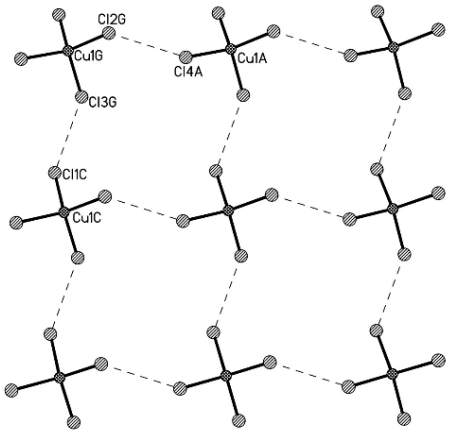


Figure 10 Rectangular lattice of $CuCl_4^{2-}$ ions, showing the magnetic exchange pathway of **4**. Viewed parallel to the *c*-axis.

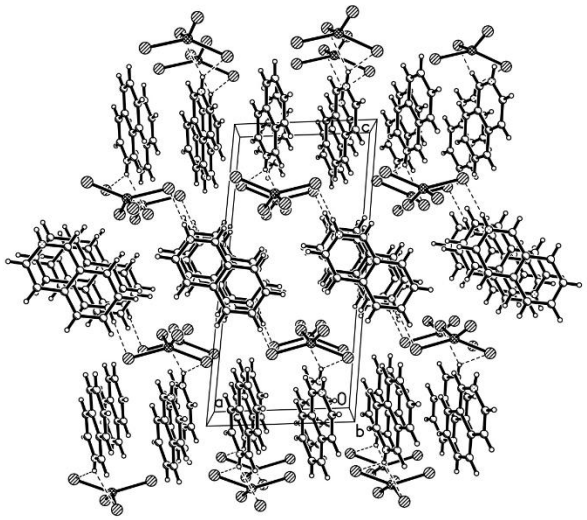

Figure 11 Packing diagram of **4** viewed along the *b*-axis.

X-ray structure of bis(isoquinolinium)tetrachlorocuprate(II) (**5**)

The asymmetric unit of **5** (Fig. 12) contains the same species as **4**. The mta at the Cu(II) ion in **5** is 134.49°, significantly closer to tetrahedral than observed in **4**. The four chloride ions are all independent (Table 2). The bond lengths are comparable to **4**. Unlike **4**, the bond angles of **5** are comparable to both bis(8-methylquinolinium) tetrachlorocuprate(II)[20] and bis(2-methylquinolinium) tetrachlorocuprate(II).[34] The two unique isoquinolinium rings hydrogen bond, through the N-H hydrogen atom, to the $CuCl_4^{2-}$ ion (Table 3). The bond angles and bond lengths of the isoquinolinium rings are unremarkable in comparison to those in **3** and **4**. The isoquinolinium ring is again highly planar, with a mean deviation of constituent atoms of 0.007 Å (N12) and 0.006 Å (N22). The planes of isoquinolinium rings are canted 77.1° with respect to one another.

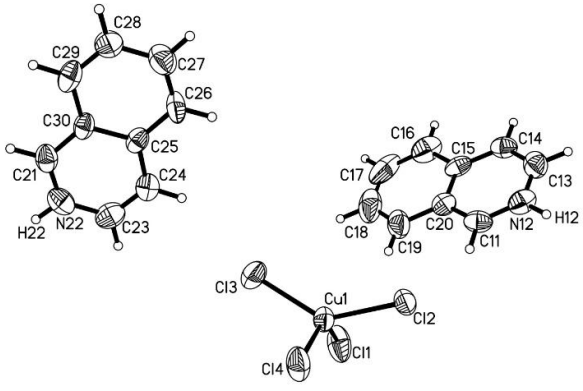


Figure 12 The thermal ellipsoid plot of **5** showing 50% probability ellipsoids. The asymmetric unit, the copper coordination sphere, and hydrogen atoms in refined positions are labeled.

The packing of the $CuCl_4^{2-}$ ions forms a structural ladder, with a Cl…$Cl_{rung}$ distance of 3.752(4)° and a Cl…$Cl_{rail}$ distance of 4.709(7)° (Fig. 13). There is an inversion center through the center of the rungs making each Cu-Cl2…Cl2 angle equivalent at 175° (Fig. 13). The torsion angle of the rung interaction is 180°, as required by symmetry. Full details of the two-halide superexchange pathway parameters are given in Table 4. The ladders run parallel to the *a*-axis. The inter-ladder distance parallel to the *b*-axis is just over 4.9 Å and parallel to the *c*-axis is just above 5.9 Å. The different orientations of the isoquinolinium rings causes the difference in inter-ladder distances (Fig. 14).

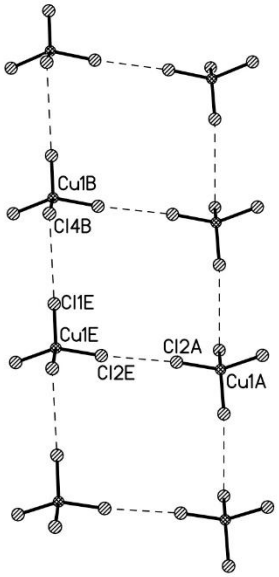


Figure 13 The ladder structure of **5** (the ladder is parallel to the *a*-axis).

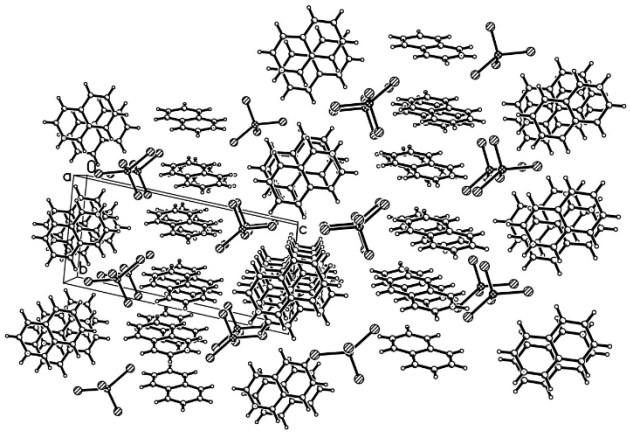

Figure 14 Packing structure of **5** viewed parallel to the *a*-axis.

X-ray structure of isoquinolinium tribromide (**6**)

The asymmetric unit of **6** contains two independent tribromide ions, and two independent isoquinolinium rings (Fig. 15). The bond lengths and angles of the two tribromide ions are shown in Table 5. These bond lengths and angles are comparable to those found in 3-bromo-1-phenyl-1,2,3,4-tetrahydro-1,4-methanoquinolizinium tribromide[35] and 1,1'-phosphinicobis[4-(dimethylamino)pyridinium tribromide.[36] There are also quinoline-containing tribromide salts, such as quinolinium hexabromoantimonate(v) tribromide,[37] and copper containing tribromide salts, such as tris(5H-pyrido[3',2':4,5]cyclopenta[1,2-b]pyridine-5-one)-copper bis(tribromide) dibromide.[38] Although the bond lengths and angles are very similar, the independent nature of the two tribromide ions is clearly seen in the packing of the ions as there are short bromide…bromide contacts between symmetry related Br5-containing ions (the shortest being 3.804(3) Å), but the Br6-containing ions only exhibit short contacts with Br5-containing ions (the shortest being 3.975(3) Å) (Fig. 16).

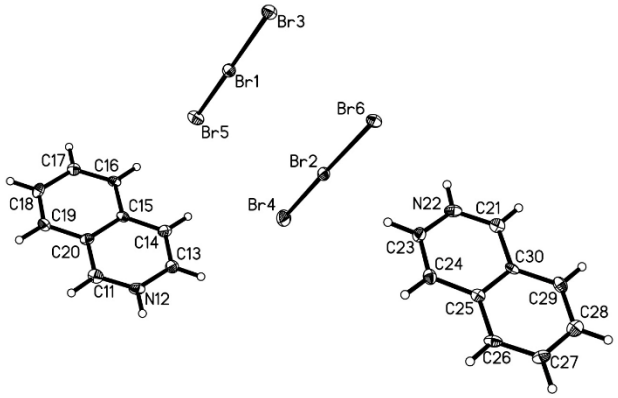


Figure 15 The thermal ellipsoid plot of **5** showing 50% probability ellipsoids. The asymmetric unit, the copper coordination sphere, and hydrogen atoms in refined positions are labeled.

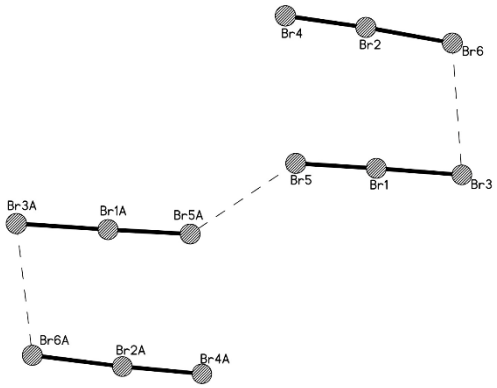


Figure 16 Packing diagram of the tribromide ions in **6**, illustrating the short bromide…bromide contacts distinguishing the tribromide ions.

Table 5 - Select bond lengths (Å) and angles (°) for **6** (Å, °).

| Compound | (**6**) |
|---|---|
| Br1-Br5 | 2.4464(7) |
| Br1-Br3 | 2.6730(7) |
| Br2-Br4 | 2.4300(7) |
| Br2-Br6 | 2.6918(7) |
| N12-C11 | 1.321(6) |
| N12-C13 | 1.365(6) |
| N22-C21 | 1.326(6) |
| N22-C23 | 1.362(6) |
| | |
| Br5-Br1-Br3 | 178.24(2) |
| Br4-Br2-Br6 | 177.99(2) |
| N12-C11-C20 | 120.1(4) |
| C11-N12-C13 | 123.6(4) |
| C14-C13-N12 | 118.9(4) |
| N22-C21-C30 | 119.7(4) |
| C21-N22-C23 | 123.4(4) |
| C24-C23-N22 | 119.9(4) |

**Magnetic susceptibility results:**

Magnetic susceptibility data were collected on compounds **1-5** over the temperature range 1.8-310 K and are shown in Figures 17-21 respectively. All show antiferromagnetic interactions, but could be best fitted using a variety of magnetic models which are summarized in Table 6.

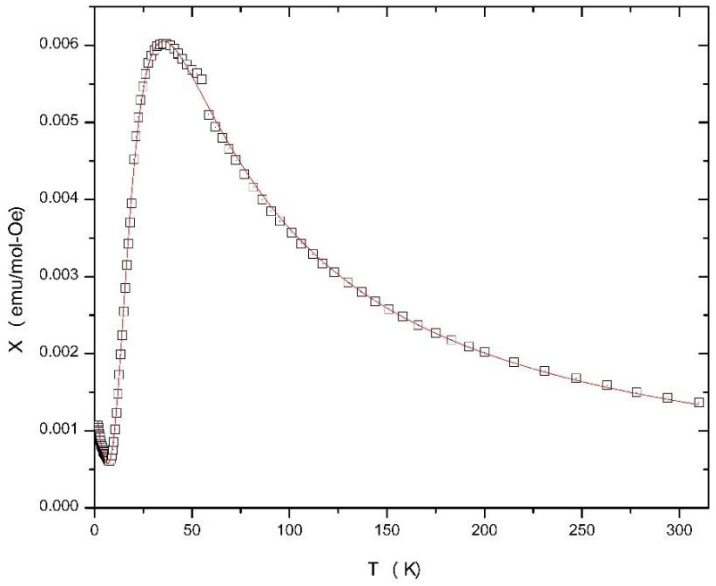


Figure 17 Magnetic susceptibility as a function of temperature for **1** in a 1 kOe field. The small anomaly near 50 K results from a trace of $O_2$ in the sample. The solid line shows the best fit to the alternating chain model.

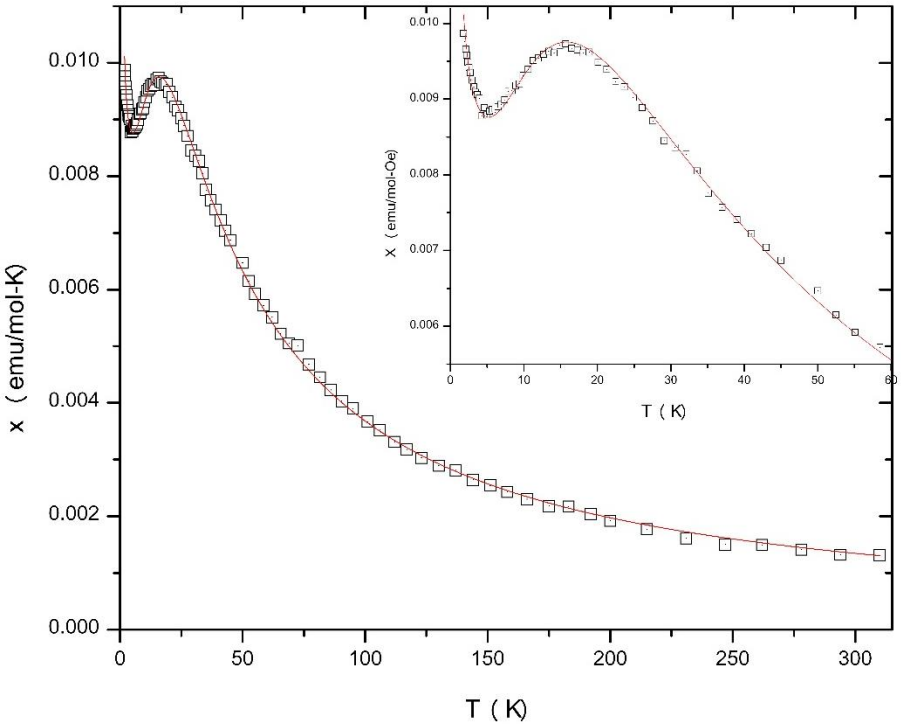


Figure 18 Magnetic susceptibility as a function of temperature for **2** in a 1 kOe field. The small anomaly near 50 K results from a trace of $O_2$ in the sample. The solid line shows the best fit to the uniform chain model. The inset shows detail of the fit in the low-temperature region.

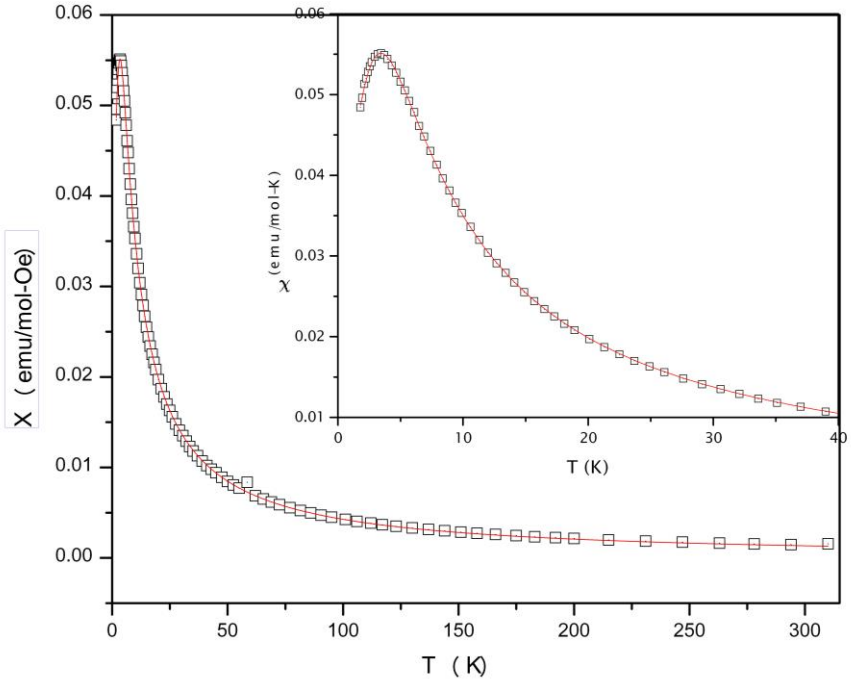


Figure 19 Magnetic susceptibility as a function of temperature for **3** in a 1 kOe field. The small anomaly near 50 K results from a trace of $O_2$ in the sample. The solid line shows the best fit to the rectangular model. The inset shows detail of the fit in the low-temperature region.

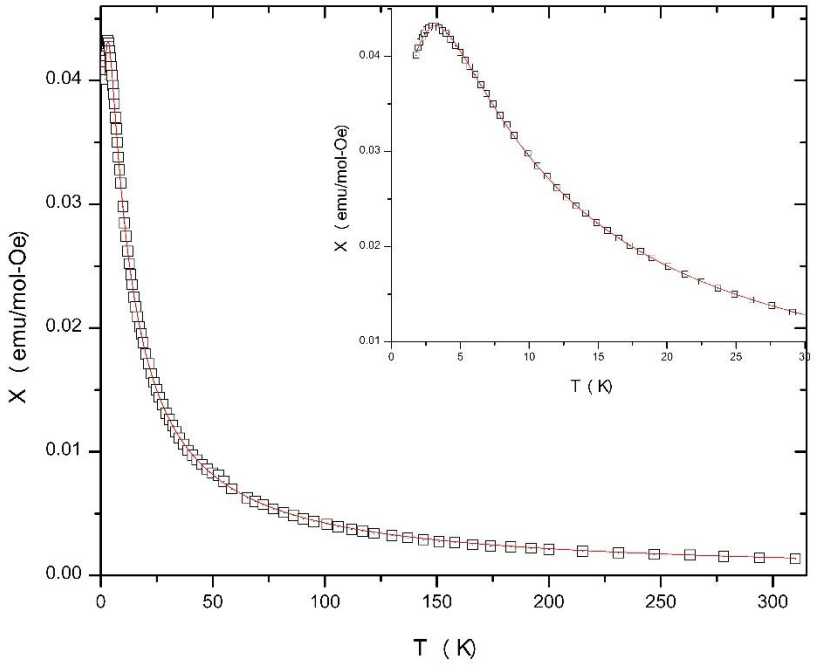


Figure 20 Magnetic susceptibility as a function of temperature for **4** in a 1 kOe field. The small anomaly near 50 K results from a trace of $O_2$ in the sample. The solid line shows the best fit to the 2D-square antiferromagnetic lattice model. The inset shows detail of the fit in the low-temperature region.

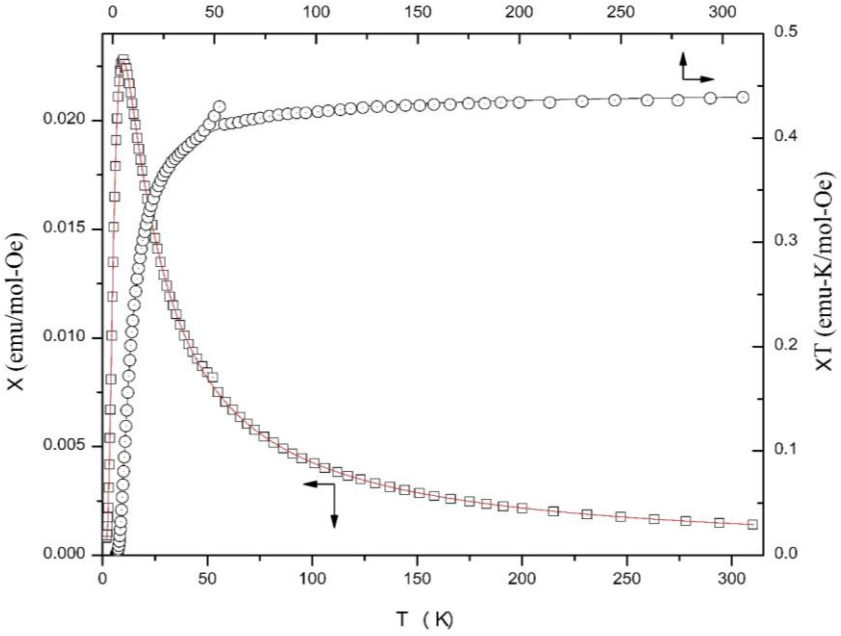


Figure 21 Magnetic susceptibility as a function of temperature for **5** (χ, (∘); χT, (□)] in a 1 kOe field. The small anomaly near 50 K results from a trace of $O_2$ in the sample. The solid line represents the best fit to the dimer model.

Table 5 - Fitted magnetic parameters for **1-5** using a variety of possible models. C = Curie constant, θ = Weiss constant, and p is the % paramagnetic impurity included in the fit. CW = Curie-Weiss correction.

| Compound | Model | C(emu-K/mol-Oe) | J (K) | J' or θ (K) | p (%) | $R^2$ |
|---|---|---|---|---|---|---|
| **1** | Dimer w/ CW | 0.411(1) | -55.3(2) | -0.81(4) | 0.58(4) | 0.9974 |
| | Strong rung ladder | 0.417(3) | -55.9(1) | -3(1) | 0.43(1) | 0.9972 |
| | Alternating Chain | 0.432(5) | -56.6(2) | 5.1(8) | 0.58(1) | 0.9974 |
| | | | | | | |
| **2** | Chain | 0.421(1) | -25.94(10) | | 1.21(2) | 0.99993 |
| | Chain w/ CW | 0.422(3) | -25.9(9) | -0.02(1.4) | 1.3(2) | 0.99995 |
| | | | | | | |
| **3** | Rectangle | 0.453(5) | -5.02(3) | -1.0(1) | 1(1) | 0.9997 |
| | | | | | | |
| **4** | Chain | 0.415(2) | -6.01(5) | | 2.7(2) | 0.9972 |
| | Chain w/ CW | 0.442(1) | -3.60(6) | -2.70(7) | 5.5(1) | 0.99995 |
| | Square | 0.438(1) | -4.24(2) | | 5.21(8) | 0.99993 |
| | | | | | | |
| **5** | Dimer | 0.445(1) | -15.82(1) | | 0.23(1) | 0.99998 |
| | Dimer w/ CW | 0.445(1) | -15.84(7) | 0.02(7) | 0.22(1) | 0.99998 |
| | Strong rung ladder | 0.445(1) | -15.81(1) | -0.02(11) | 0.22(1) | 0.99997 |

**Discussion**

The correlation between the supposed magnetic lattice derived from the short contacts seen in the crystal structures of **1-5** is in general quite good, with the distinct exception of compound **1**. In **1**, short Cu…Br contacts between molecular units leads to the formation of halide bi-bridged chains. However, all attempts to fit the data to the uniform linear chain model resulted in unphysical values for the Curie constant and magnetic exchange constant. Surprisingly, the data could be fit very well by a simple dimer model with a small Curie-Weiss correction for interdimer interactions, via the alternating chain model, or via the strong rung ladder model. The agreement between the values for the Curie constant, J and the paramagnetic impurity phase clearly support an arrangement of packed dimers, but the crystal structure clearly suggests a uniform chain. The most likely explanation is a low-temperature phase transition (below 150 K

where the crystal structure was obtained), such as a Spin-Peierls transition which would agree well with the fit to the alternating antiferromagnetic chain. However, no anomaly is seen in the magnetic data to suggest such a transition. This could mean that the transition is second order, or that the difference in the exchange parameters is small enough to not be detected via susceptibility measurements. More detailed study and a much lower temperature crystal structure will be necessary to fully understand the interactions in this material.

Data for compound **2** are well fit by the uniform chain model with J ~ -26 K. The data are equally well fit by the uniform chain model with a Curie-Weiss term to account for possible interchain interactions, but the value of θ thus obtained is zero within experimental error. This suggests that the chains are very well isolated in the lattice and supports the proposal that **2** has a structure very similar to that of **1**, but it must not undergo the low temperature phase transition which appears to exist for **1**.

The crystal structure of compound **3** shows two short Br…Br contacts, ~ 3.9 and 4.1Å, parallel to the *b*- and *a*- axes respectively, which generate a rectangular magnetic lattice. The data are well fit by that model with values of -5 and -1 K for J and J'. The strength of magnetic exchange via the two-halide pathway is known to vary depending up the inter-halogen distance as well as the Cu-Br…Br angles[12] with the Br…Br distance being the primary factor in low-symmetry cases such as the bi-halide linkages in **3** (Table 4). Thus, the fitted values are in good agreement with the superexchange pathways suggested by the crystal structure.

The two polymorphs of $(iQuinH)_2CuCl_4$ present an interesting case. Due to the similarity in color (one is more orange, the other more yellow) and crystal habit, one could easily miss the fact that there are two species. We have observed this phenomena before in the case of the two polymorphs of Cu(2-chloro-3-methylpyridine)$Cl_2$, although the fact that the colors in the case of those polymorphs are also one more orange and one more yellow is coincidental since both are 5-coordinate structures.[39] The initially formed polymorph, **4**, appears to be a kinetic product of the reaction as over time, if left in the mother liquor, crystals of **4** will redissolve and give way to crystals of **5**. The structures of the molecular units differ primarily in the degree of distortion of the tetrachlorocuprate ion, with **4** being much more highly flattened (mean trans angle ~144°) than is seen in **5** (134°). This results in different packing arrangements where **4** packs in a rectangular motif, similar to **3**, but with the two Cl…Cl contact distances being nearly identical (3.78 Å and 3.83 Å). Given the similarity in the two potential superexchange pathways (see Table 4), the magnetic susceptibility data for **4** were fit to the two-dimensional square lattice model which gave excellent agreement with an intralayer exchange value of -4.24(2) K (Figure 20). The data can be fit equally well by the uniform chain model with a Curie-Weiss correction for interchain interactions with values of J = -3.60(6) K and θ = -2.70(7) K. The Curie-Weiss approximation is only valid when θ is a small percentage of the principle magnetic exchange constant.[40] In this case, θ is 75% of the value of J which while it suggests that the approximation is not valid, the nearly equal values of J and θ support the results from the square layer fit.

Finally, polymorph **5** showed a potential ladder structure, but with very different Cl…Cl contact distances (rung ~ 3.7 Å, rail ~ 4.7 Å) suggesting that the rail interactions would be weak, if they were observable at all. Indeed, the susceptibility data for **5** were fit virtually identically by the dimer model (with or without Curie-Weiss correction) and the strong-rung ladder model. In the latter two cases, θ and J' were fit to zero within experimental error. The magnetic dimers in the sample are very well isolated.

Compound **6** was unexpected, but does provide important support for reactions previously reported. On a few occasions, we[41] and others[42] have observed bromination of aromatic rings during the preparation of $CuBr_2$ salts in HBr solution. It has been proposed to occur via air-oxidation of bromide ion to produce $Br_2$ which can subsequently undergo an electrophilic addition to the aromatic ring. However, there has been no direct observation of $Br_2$ formation. The observation of the tribromide ion in **6**, isolated as a by-product of the synthesis of **3** in aqueous HBr is most easily explained by the formation of $Br_2$, again presumably via air-oxidation of bromide, and its subsequent reaction with bromide ion. Thus, it provides further support for the proposed formation of these brominated by-products. The compound can be synthesized directly from the reaction of isoquinoline with $Br_2$ and HBr and both the synthesis and crystal structure have been recently reported.[43]

## Conclusions

In conclusion, it is clear that isoquinoline provides a rich assortment of possible complexes and salts with copper halides and with a variety of structures not seen in the corresponding compounds of quinoline. Copper halide chemistry continues to show great malleability about the Cu(II) ion itself and provides room for further investigation. Work is currently underway to prepare the related compounds with additional transition metal ions including Ni(II), Co(II) and Mn(II).

## Conflicts of interest

There are no conflicts to declare.


## Acknowledgements

MTK is grateful for partial support from PCISynthesis Inc.


## References


[1] M. Kastner, R. Birgeneau, G. Shirane and Y. Endoh, *Rev. Mod. Phys.*, 1998, **70**, 897.

[2] R. D. Willett, D. Gatteschi and O. Kahn, 1985, *Magneto-structural correlations in exchange coupled systems.* United States: D Reidel Publishing Co.

[3] J. Mroziński, *Coord. Chem. Rev.*, 2005, **249**, 2534.

[4] U. Geiser and R. D. Willett, *J. Appl. Phys.*, 1984, **55**, 2407.

[5] C. Zanchini and R. D. Willett, *Inorg. Chem.*, 1990, **29**, 3027.

[6] J. Masternak, M. Zienkiewicz-Machnik, M. Kowalik, A. Jabłońska-Wawrzycka, P. Rogala, A. Adach and B. Barszcz, *Coord. Chem. Rev.*, 2016, **327-328**, 242.

[7] L. Ouahab, *Coord. Chem. Rev.*, 1998, **178**, 1501.

[8] R. L. Carlin, *Magnetochemistry*, 1986, Springer-Verlag Berlin Heidelberg.

[9] J. A. Schlueter, H. Park, G. J. Halder, W. R. Armand, C. Dunmars, K. W. Chapman, J. L. Manson, J. Singleton, R. McDonald and A. Plonczak, *Inorg. Chem.*, 2012, **51**, 2121.
[10] S. Haddad, A. Vij and R. D. Willett, *J. Chem. Crystallog.*, 2003, **33**, 245.
[11] A. Kelley, S. Nalla and M. R. Bond, *Acta Crystallogr. Section B*, 2015, **71**, 48.
[12] M. M. Turnbull, C. P. Landee and B. M. Wells, *Coord. Chem. Rev.*, 2005, **249**, 2567.
[13] G. W. Tremelling, B. M. Foxman, C. P. Landee, M. M. Turnbull and R. D. Willett, *Dalton Trans.*, 2009, 10518.
[14] J. Ribas-Ariño, J. J. Novoa and J. S. Miller, *J. Mat. Chem.*, 2006, **16**, 2600.
[15] R. T. Butcher, M. M. Turnbull, C. P. Landee, A. Shapiro, F. Xiao, D. Garrett, W. T. Robinson and B. Twamley, *Inorg. Chem.*, 2009, **49**, 427.
[16] D. E. Lynch and I. McClenaghan, *Acta Crystallogr. Section E:* 2002, **58**, m551.
[17] J. Valdés-Martínez, O. Munoz and R. A. Toscano, *Acta Crystallogr. Section E:* , 2005, **61**, m1590.
[18] D. Wyrzykowski, Z. Warnke, R. Kruszyński, J. Kłak and J. Mroziński, *Trans. Met. Chem.*, 2006, **31**, 765.
[19] D. Wyrzykowski, A. Sikorski, T. Lis, A. Konitz and Z. Warnke, *Acta Crystallogr. Section E:*, 2006, **62**, m1737.
[20] K. Edwards, S. N. Herringer, A. R. Parent, M. Provost, K. C. Shortsleeves, M. M. Turnbull and L. N. Dawe, *Inorg. Chim. Acta*, 2011, **368**, 141.
[21] D. Wyrzykowski, A. Sikorski, A. Konitz and Z. Warnke, *Acta Crystallogr. Section E:*, 2006, **62**, m3562.
[22] L. Luis, P. Martin-Zarza, P. Gili, C. Ruiz-Perez, M. Hernandez-Molina and X. Solans, *Acta Crystallogr. Section C:* , 1996, **52**, 1441.
[23] R. Ivaniková, R. Boča, L. Dlháň, H. Fuess, A. Mašlejová, V. Mrázová, I. Svoboda and J. Titiš, *Polyhedron*, 2006, **25**, 3261.
[24] J. Miklovič, A. Packová, P. Segl'a, J. Titiš, M. Koman, R. Boča, V. Jorík, H. Krekuska and D. Valigura, *Inorganica Chimica Acta*, 2015, **429**, 73.
[25] C. Sharma, V. Mishra and K. Samuel, *Acta Chim. Hung.*, 1990, **127**, 865.
[26] C.P. Landee, M.M. Turnbull, *J. Coord. Chem.*, 2014, **67**, 375.
[27] H. Ohara, A. Kobayashi and M. Kato, *Compt. Rend. Chim.*, 2015, **18**, 766.
[28] K. Al Sarraj, J. Gouteron, S. Jeannin and Y. Jeannin, *Acta Crystallogr Section C:*, 1987, **43**, 1261.
[29] W. Clegg and B. Straughan, *Acta crystallogr. Section C:*, 1989, **45**, 1992.
[30] P. Šegedin, U. Dolničar, M. Čuskić, Z. Jagličić, A. Golobič and B. Kozlevčar, *Acta Chim. Slov.*, 2008, **55**. 992.
[31] J. A. van Ooijen, J. Reedijk, E. J. Sonneveld and J. W. Visser, *Trans. Met. Chem.*, 1979, **4**, 305.
[32] B. D. James, J. Mrozinski, J. Klak, B. W. Skelton and A. H. White, *Z. Anorg. Allg. Chem.*, 2009, **635**, 317.
[33] E. Govindan, S. Thirumurugan, K. Rajkumar, K. Anbalagan and A. Subbiah Pandi, *Acta Crystallogr. Section E:* , 2014, **70**, m303.
[34] S. Jin and D. Wang, *J. Coord. Chem.*, 2012, **65**, 3188.
[35] H. E. Zimmerman and P. Wang, *J. Org. Chem.*, 2002, **67**, 9216.
[36] P. Rovnaník, L. Kapicka, J. Taraba and M. Cerník, *Inorg. Chem.* 2004, **43**, 2435.
[37] S.L.Lawton, E.R.McAfee, J.E.Benson and R.A.Jacobson *Inorg. Chem.* 1873, **12**, 2939.
[38] R.Babu, G.Bhargavi and M.V.Rajasekharan *Eur. J. Inorg. Chem*. 2015, 4689.
[39] S.N. Herringer, C.P. Landee, M.M. Turnbull, J. Ribas-Ariño, J.J. Novoa, M. Polson, J.L. Wikaira, J.L *Inorg. Chem.* 2017, **56**, 5441.
[40] R.T. Butcher, C.P. Landee, M.M. Turnbull and F. Xiao, *Inorg. Chim. Acta* 2008, **361**, 3654.
[41] C.A. Krasinski, B.L. Solomon, F.F. Awwadi, C.P. Landee, M.M. Turnbull and J. L. Wikaira *J. Coord. Chem*. 2017, **70,** 914.
[42] a) H. Place, R.D. Willett. *Acta Cryst. C: Cryst. Struct. Comm.*, 1987, **C43**, 1497. b) F. Gallou, J.T. Reeves, Z. Tan, J. Song, N.K. Yee, C. Harcken, P. Liu, D. Thomson, C.H. Senanayake, *Synlett*, 2007, 211.
[43] I.D. Gorokh, S.A. Adonin, M.N. Sokolov, P.A. Abramov, I.V. Korolkov, E.Yu. Semitut, V.P. Fedin, *Inorg. Chim. Acta*, 2018, **469**, 583.